The Plant Cell, Vol. 24: 3838–3852, September 2012, www.plantcell.org

Two Direct Targets of Cytokinin Signaling Regulate Symbiotic Nodulation in *Medicago truncatula*[W][OA]

Federico Ariel,[a,b,1] Marianne Brault-Hernandez,[a,1] Carole Laffont,[a] Emeline Huault,[a] Mathias Brault,[a,c] Julie Plet,[a,2] Michael Moison,[a] Sandrine Blanchet,[a,3] Jean Laurent Ichanté,[d] Mireille Chabaud,[e] Sébastien Carrere,[e] Martin Crespi,[a] Raquel L. Chan,[b] and Florian Frugier[a,4]

[a] Institut des Sciences du Végétal, Centre National de la Recherche Scientifique, F-91198 Gif-sur-Yvette cedex, France
[b] Instituto de Agrobiotecnología del Litoral, Consejo Nacional de Investigaciones Científicas y Técnicas, Universidad Nacional del Litoral, Ciudad Universitaria, CP 3000 Santa Fe, Argentina
[c] Université Paris Diderot, Sorbonne Paris Cité, F-75205 Paris cedex 13, France
[d] Gif/Orsay DNA MicroArray Platform and Centre de Génétique Moléculaire, Centre National de la Recherche Scientifique, F-91198 Gif-sur-Yvette cedex, France
[e] Laboratoire des Interactions Plantes Micro-organismes, Unité Mixte de Recherche, Centre National de la Recherche Scientifique, Institut National de la Recherche Agronomique, 2594/441, F-31320 Castanet-Tolosan, France

Cytokinin regulates many aspects of plant development, and in legume crops, this phytohormone is necessary and sufficient for symbiotic nodule organogenesis, allowing them to fix atmospheric nitrogen. To identify direct links between cytokinins and nodule organogenesis, we determined a consensus sequence bound in vitro by a transcription factor (TF) acting in cytokinin signaling, the nodule-enhanced *Medicago truncatula* Mt RR1 response regulator (RR). Among genes rapidly regulated by cytokinins and containing this so-called RR binding site (RRBS) in their promoters, we found the nodulation-related Type-A RR Mt *RR4* and the Nodulation Signaling Pathway 2 (*NSP2*) TF. Site-directed mutagenesis revealed that RRBS *cis*-elements in the *RR4* and *NSP2* promoters are essential for expression during nodule development and for cytokinin induction. Furthermore, a microRNA targeting *NSP2* (miR171 h) is also rapidly induced by cytokinins and then shows an expression pattern anticorrelated with *NSP2*. Other primary targets regulated by cytokinins depending on the Cytokinin Response1 (CRE1) receptor were a cytokinin oxidase/dehydrogenase (*CKX1*) and a basic Helix-Loop-Helix TF (*bHLH476*). RNA interference constructs as well as insertion of a *Tnt1* retrotransposon in the *bHLH* gene led to reduced nodulation. Hence, we identified two TFs, NSP2 and bHLH476, as direct cytokinin targets acting at the convergence of phytohormonal and symbiotic cues.

INTRODUCTION

Plant hormones play crucial roles in regulating organogenesis, and cytokinins have been shown to affect cell proliferation, elongation, differentiation, or senescence depending on the developmental context. In *Arabidopsis thaliana*, cytokinins are perceived through an extracellular Cyclase/Histidine Kinase-Associated Sensing Extracellular (CHASE) domain present in Cytokinin Response1/Authentic Histidine Kinase4 (CRE1/AHK4) transmembrane receptors as well as two other related sensors (AHK2 and AHK3; Werner and Schmülling, 2009). Downstream of these cytokinin receptors, a Histidyl-Aspartyl multistep phosphorelay is initiated, leading to the activation of Type-B response regulators (RRs). These plant Myb-related transcription factors (TFs; Stracke et al., 2001) can regulate cytokinin primary response genes, such as the Type-A RRs (Brandstatter and Kieber, 1998; D'Agostino et al., 2000; Sakai et al., 2000, 2001; Hwang and Sheen, 2001). DNA binding sites were identified for several *Arabidopsis* Type-B RRs (ARR1, ARR2, ARR10, and ARR11), but only a short consensus RR binding sequence was identified [5′-(A/G)GAT(T/C)-3′] (Sakai et al., 2000; Lohrmann et al., 2001; Hosoda et al., 2002; Imamura et al., 2003), preventing the reliable identification of transcripts directly regulated by these TFs. In addition, it was suggested that an extended sequence is likely required to allow specific interaction of each RR in a promoter context, notably to discriminate between various GOLDEN2/ARRs/PSR1/PHR1 (GARP)-type TFs (Taniguchi et al., 2007). In parallel, transcriptomic analyses performed in *Arabidopsis* revealed a wide variety of genes responding rapidly to exogenous cytokinins in seedlings of the wild type, transgenics, or mutants affected in cytokinin level or sensitivity (Hoth et al., 2003; Rashotte et al., 2003; Kiba et al., 2004; Brenner et al., 2005; Kiba et al., 2005; Rashotte et al., 2006; Lee et al., 2007; Taniguchi et al., 2007). Taniguchi et al. (2007) notably identified, based on the combined analysis of an inducible Type-B RR (ARR1) protein lacking its phosphoreceiver domain (ΔDDK), an *arr1* mutant, and cycloheximide treatments, 17 genes regulated by cytokinins independently of

[1] These authors contributed equally to this work.
[2] Current address: Centre d'Etudes Atomiques, F-13108 Cadarache, France.
[3] Current address: Centre d'Etudes Atomiques, F-38054 Grenoble, France.
[4] Address correspondence to frugier@isv.cnrs-gif.fr.
The author responsible for distribution of materials integral to the findings presented in this article in accordance with the policy described in the Instructions for Authors (www.plantcell.org) is: Florian Frugier (frugier@isv.cnrs-gif.fr).
[W] Online version contains Web-only data.
[OA] Open Access articles can be viewed online without a subscription.
www.plantcell.org/cgi/doi/10.1105/tpc.112.103267

de novo protein synthesis. ARR1 interaction with the promoter of one of these putative targets, coding for IAA3/SHY2, was validated by chromatin immunoprecipitation (ChIP), and this direct regulation of the auxin response by cytokinins was shown to control the balance between cell proliferation and differentiation at the root meristem transition zone (Dello Ioio et al., 2008).

Arabidopsis roots do not develop symbiotic interactions, whereas legume plants have the ability to interact with nitrogen-fixing bacteria under nitrogen starvation conditions. In response to a specific bacterial microsymbiont (e.g., *Sinorhizobium meliloti* for the model legume *Medicago truncatula*), a new organ is formed on host legume roots (the nitrogen-fixing nodules), and cytokinins are crucial for this organogenesis (Frugier et al., 2008). Systematic RNA interference (RNAi) targeting of the different *M. truncatula* cytokinin receptors revealed that the Cytokinin Response1 (CRE1) His kinase regulates nodule formation (Gonzalez-Rizzo et al., 2006). Similarly, the *Lotus japonicus hyperinfected1* (*hit1*) mutant carrying a loss-of-function mutation in the *L. japonicus Histidine Kinase1* (*LHK1*) gene (functionally related to *CRE1*) showed a strongly reduced nodulation (Murray et al., 2007). Interestingly, the *L. japonicus spontaneous nodule formation2* (*snf2*) gain-of-function mutation affecting the same LHK1 receptor led to the formation of nodules in the absence of rhizobia (Tirichine et al., 2007). This result indicates that cytokinins are necessary and sufficient to activate cortical cell divisions and nodule organogenesis.

To search for genes directly regulated by the cytokinin cue and acting in legume root nodule development, we combined a transcriptomic analysis of *M. truncatula* root response to cytokinins with a systematic evolution of ligands by exponential enrichment (SELEX) approach for the nodule-associated RR Mt RR1 (Gonzalez-Rizzo et al., 2006). This allowed us to determine a large 12-bp RR binding site (RRBS), which was retrieved in promoters of several cytokinin-regulated genes, including two genes linked to nodulation: *RR4*, a Type-A RR (Plet et al., 2011), and the *NSP2* TF (Kaló et al., 2005; Heckmann et al., 2006). These RRBSs were essential for cytokinin induction and symbiotic expression of these genes and allowed us to further identify direct targets of cytokinins acting in legume roots, including a new basic Helix-Loop-Helix (bHLH) TF, *bHLH476*. Downregulating bHLH476 expression, using either RNAi constructs or an insertional mutant, resulted in a reduced nodulation. Therefore, *NSP2* and *bHLH476* are two direct targets of cytokinins acting positively in symbiotic nodulation.

RESULTS

Cytokinin Target Genes and Functional Pathways Acting in *M. truncatula* Root Apices

To gain knowledge about cytokinin primary response genes in legume roots and nodules, we first developed a transcriptomic approach focused on the root apical region containing the zone required for rhizobial symbiotic interactions. This allowed us to identify transcripts regulated by a short-term exogenous cytokinin treatment (10^{-7} M of benzyl amino purine [BAP] for 1 h; see Supplemental Data Set 1 online) in this root region. The most significant differentially expressed functional categories were the flavonoid (see Supplemental Figures 1A and 1B online) and gibberellin (GA) metabolisms (see Supplemental Figure 1C online; $P < 0.001$, Fisher's exact test, shown in Supplemental Table 1 online). Two enzymatic families were also very significantly affected ($P < 0.002$), the UDP glucosyl and glucuronyl transferases and the cytochrome P450 families (see Supplemental Figure 1D online), with several members related to flavonoid or cytokinin metabolism (i.e., zeatin O-glycosyltransferases and CYP735-A2 cytochrome P450 enzymes). Finally, a significant enrichment was observed for two families of TFs: bHLH and

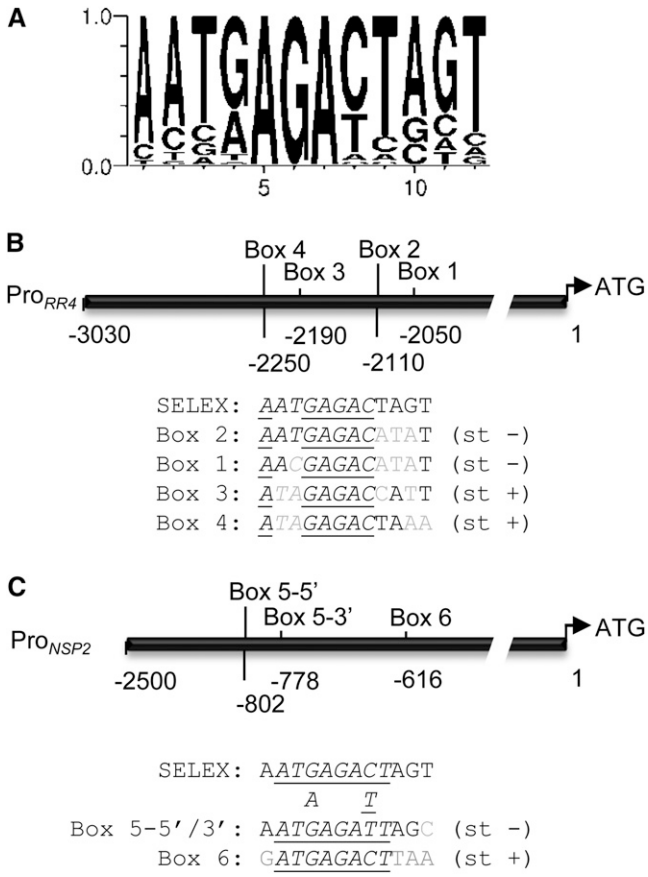

Figure 1. RRBSs in the Promoter of the *RR4* and *NSP2* Nodulation-Related Genes.

(A) Consensus sequence bound by the RR1 BD identified by SELEX. Numbers on the *x* and *y* axes, respectively, represent nucleotide positions and the frequency of occurrence (shown by letter size normalized from 0 to 1) of each nucleotide for each position (WebLogo; Crooks et al., 2004).

(B) and **(C)** Schematic diagram of *RR4* **(B)** and *NSP2* **(C)** promoter regions. The RRBS *cis*-element variants (boxes 1 to 6) are indicated. Alignment to the major SELEX consensus is shown below each promoter diagram. Gray indicates nonconserved nucleotides, underlined indicates conserved nucleotides between all boxes of each promoter, italics indicates 8-bp RRBS core, and st + or str − indicates DNA strand of sequences shown.

APETALA2/Ethylene Response Factor/Ethylene-Responsive Element Binding Protein (AP2/ERF/EREBP). The latter family was previously linked to cytokinin responses through the identification of cytokinin response factors (CRFs) (Rashotte et al., 2006). A BLASTX analysis revealed, however, that none of the identified AP2/ERF TFs regulated by cytokinins in *M. truncatula* roots were closely related to CRFs.

Overall, this transcriptomic analysis allowed us to identify genes rapidly regulated by cytokinins in legume roots, highlighting the enrichment for transcripts related to cytokinin, GA, and flavonoid metabolisms as well as for bHLH and AP2/ERF TFs.

Identification of a RRBS *cis*-Element Revealed New Candidate Cytokinin Primary Response Genes

To identify direct molecular links between cytokinin regulation of gene expression and nodule organogenesis, we searched for targets of Mt *RR1*, a RR that is highly expressed during nodulation (Gonzalez-Rizzo et al., 2006) and that is able to interfere with root cytokinin sensitivity when expressed in *Arabidopsis* (see Supplemental Figure 2 online). To determine its DNA binding site, a region containing the RR1 DNA binding domain (BD) was expressed in *Escherichia coli* as a fusion with glutathione-*S*-transferase (GST) and purified by affinity chromatography. Seven rounds of PCR-assisted binding site selection (SELEX) were performed, and because no additional improvement was detected in an eighth round, 38 individual clones were randomly selected for sequencing. Every clone contained an AGA (or TCT) core, used as a reference to align all the sequences (see Supplemental Figure 3 online). Eighteen clones were identical, and the others were remarkably similar around the core sequence, leading to the following 12-bp consensus, referred to as the Mt RR1 RRBS consensus: 5′-AAT(G/A)AGA(C/T)TAGT-3′ [or the reverse complement 5′-ACTA(G/A)TCT(C/T)ATT-3′] (Figure 1A).

By combining these data, we developed a bioinformatic workflow to identify, among genes rapidly regulated by cytokinins in legume roots, those having a conserved RRBS core of at least 8 bp in their promoters. Comparison between 2.5-kb promoters of a similar number of randomly chosen cytokinin- and non–cytokinin-regulated genes (n = 150) revealed enrichment for multiple RRBS consensus cores in promoters of cytokinin-regulated genes (4% versus 1.5%). Promoters having more than two potential RRBS *cis*-elements corresponded to 13 genes upregulated by cytokinins, including *RR4* and two TF-encoding genes from the NAM and GRAS families (Table 1; see Supplemental Data Set 2 online). RR4 is a Type-A RR previously characterized as a cytokinin primary response gene acting early in *Medicago* nodule organogenesis (Vernié et al., 2008; Plet et al., 2011). Analysis of a ~3-kb region upstream of its ATG revealed four 12-bp regions highly similar to the RRBS consensus identified by SELEX, present between 1.9 to 2.2 kb before the predicted RR4 start codon and arranged in two tandems (Figure 1B, boxes 1 to 4). Six nucleotide positions identical among all four boxes corresponded to the consensus sequence identified by SELEX, and two to three nucleotides were additionally conserved on the different boxes (Figure 1B). Overall, each box showed a 66 to 75% identity (i.e., 8 to 9 bp out of 12) to the RRBS consensus. Strikingly, the GRAS TF identified was the *NSP2* gene, which is crucial for symbiotic nodulation (Kaló et al., 2005; Heckmann et al., 2006). This promoter contains three RRBS *cis*-elements, a tandem of two identical boxes and another RRBS variant (Figure 1C, boxes 5 and 6). Overall, identity of eight to 11 bases was found between these boxes and the 12-bp RRBS.

A second screen was then performed with the RRBS core from each of the two nodulation-related genes that was the most closely related to the SELEX consensus (Figures 1B and 1C; see Supplemental Data Set 2 online, boxes 2 and 5 highlighted in green and yellow, respectively). Three additional TFs encoding genes from GRAS, LOB, and bZIP families were identified among

Table 1. Selected Candidate Cytokinin-Regulated Genes with RRBS *cis*-Elements in Their Promoters

Genomic ID	Box 2	Box 5	Total No. of 8-bp Core RRBS	TIGR Database ID	FC BAP versus Control	Adjusted P-Value	Description
Medtr5g037580.1	1	0	4	TC103991	11.12	3E−05	RR Mt *RR4*
Medtr3g097800.1	0	2	3	TC98097	3.98	6E−04	GRAS TF (Mt *NSP2*)
Medtr1g135030.1	1	0	2	TC98397	3.46	0.004	LOB TF
Medtr5g014710.1	0	1	2	TC95476	1.92	0.027	bHLH TF (Mt *bHLH476*)
Medtr2g116970.1	1	0	2	TC109615	1.9	0.001	GRAS TF
Medtr5g069060.1	1	1	3	TC103195	1.76	5E−04	Pathogenesis-related and ERF TF
Medtr4g097530.1	1	0	2	AW684462	1.73	2E−04	bZIP TF
Medtr7g005040.1	0	0	4	TC95048	1.6	6E−04	NAM TF
Medtr4g135740.1	0	2	2	TC95247	1.78	0.035	GST
Medtr1g019530.1	0	1	2	TC95407	1.63	0.007	Cytokinin oxidase (Mt *CKX1*)

List of all genes encoding TFs induced in response to cytokinins (10^{-7} M of BAP for 1 h) in root apices (FC > 1.5, adjusted P < 0.05) and whose promoters (2.5 kb) contain at least three 8-bp core RRBSs or at least two RRBSs of which one is a box 2 or a box 5. Homologs of candidate cytokinin primary response genes previously reported in *Arabidopsis* (Tanigushi et al., 2007) are also indicated at the end of the table. Included for each gene: a genomic accession number, the number of box 2, box 5, and the total number of RRBS present in their promoter, a TC accession number (TIGR database), the FC and adjusted P-value, and a functional annotation.

cytokinin-regulated genes having at least one box 2 core and an additional RRBS core sequence (Table 1). Similarly, promoters from a bHLH TF and two homologs of potential *Arabidopsis* cytokinin primary response genes (Taniguchi et al., 2007) had a box 5 core associated with an additional RRBS core (Table 1).

Altogether, these different analyses led to the identification of 56 candidate cytokinin primary response genes, among which only two were previously reported in *Arabidopsis*. Seven TF-encoding genes upregulated by cytokinins were notably identified, and one, very interestingly, corresponded to *NSP2*, a known regulator of symbiotic nodulation.

Expression of *RR4* and *NSP2* Symbiotic Genes in Nodule Primordia and Cytokinin-Treated Roots Depends on RRBS *cis*-Elements

We then focused our interest on the two genes previously linked to legume symbiotic nodulation, *RR4* and *NSP2*. ChIP followed by real-time PCR (ChIP-qPCR) was used first to validate in vivo the direct interaction of these promoters with RR1 (Figure 2A). In addition, electrophoretic mobility shift assays (EMSAs) showed that RR1 was able to recognize in vitro the six RRBS sequence variants present in these promoters (boxes 1 to 6, Figure 2B). When the central GAGA/TCTC core of the SELEX consensus was replaced by a CAGT/ACTG sequence, RR1 binding was abolished, indicating a specific in vitro interaction. Interestingly, the main sequence obtained by SELEX as well as the box most alike from the *RR4* promoter (box 2) showed the best binding compared with the other boxes (Figure 2B). This result was further validated by competition EMSA performed with the different boxes (see Supplemental Figure 4 online).

Using promoter-β-glucuronidase (*GUS*) fusions and site-directed mutagenesis, the significance of the *RR4* promoter box 2, which is most closely related to the SELEX consensus and efficiently bound in vitro by RR1, was analyzed in vivo (Figure 2C, left, $Pro_{RR4\text{-}box\ 2*}$). This *cis*-element was essential to activate a *GUS* transcriptional fusion in response to cytokinins, indicating that the box 2 RRBS is a bona fide *cis*-element of the *RR4* primary response gene. RR1 in vitro binding efficiency was similar for the two RRBS variants identified in the *NSP2* promoter (boxes 5 and 6, Figure 2B); therefore, a simultaneous mutagenesis of the three *cis*-elements was performed, revealing their requirement

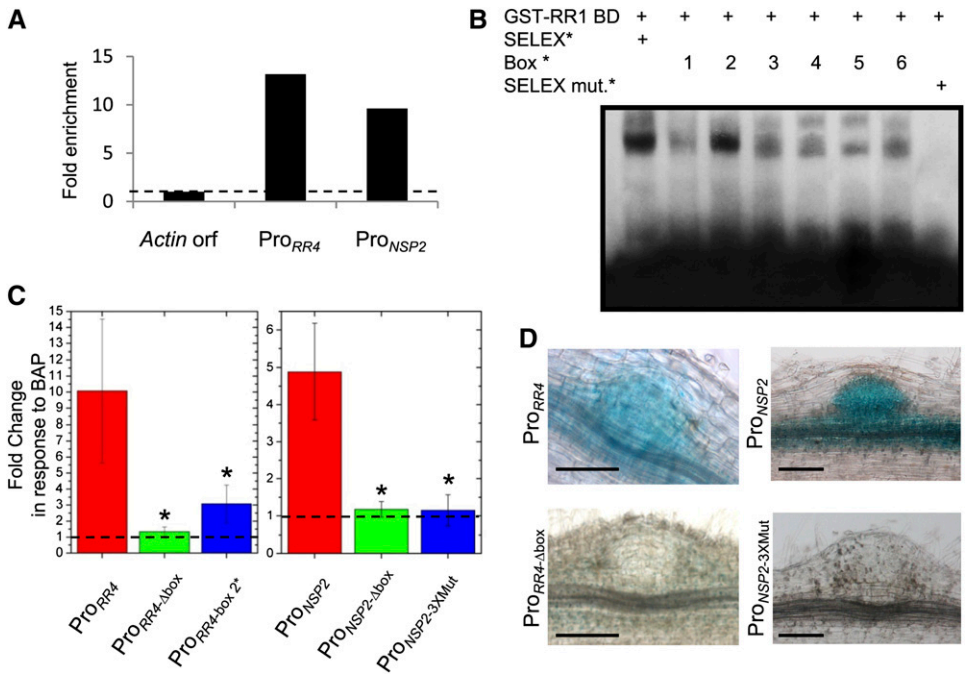

Figure 2. RRBS *cis*-Elements in the *RR4* and *NSP2* Promoters Are Required for Cytokinin Regulation and Expression in Nodule Primordia.

(A) ChIP-qPCR of RR1 binding to *RR4* and *NSP2* promoters. The *Actin11* ORF was used as a negative control, and IP values were normalized for each gene against the input genomic DNA. Ratios with *Actin11* were calculated to visualize RR1 binding fold enrichment ($n > 30$ independent transgenic roots/construct).

(B) EMSA analysis of the RR1 binding to different 12-bp oligonucleotides labeled with [α-^{32}P] dATP (indicated by asterisk): the major SELEX consensus, boxes 1 to 4 (*RR4* promoter), boxes 5 and 6 (*NSP2* promoter), and a SELEX consensus where the central GAGA core was replaced by a ACTG sequence (SELEX mut.).

(C) Fluorometric quantification of GUS activity in roots expressing Pro_{RR4}:*GUS* (left) or Pro_{NSP2}:*GUS* (right) fusions after treatment with 10^{-7} M of BAP for 3 h. Error bars represent SD ($n > 20$ independent transgenic roots). A Kruskal-Wallis test was performed to assess significant differences ($\alpha < 0.05$).

(D) Histochemical staining of GUS activity in nodule primordia expressing Pro_{RR4}:*GUS* (left) or Pro_{NSP2}:*GUS* (right) fusions. In [**(C)** and **(D)**], $Pro_{RR4\text{-}\Delta box}$:GUS and $Pro_{NSP2\text{-}3XMut}$:GUS fusions were also used (see Methods for details).

Bars in **(D)** = 50 μm.

for cytokinin induction (Figure 2C, right, $Pro_{NSP2\text{-}3Xmut}$). Finally, because both *cre1* and *nsp2* mutants are defective in early nodule organogenesis (Kalo et al., 2005; Plet et al., 2011), we analyzed the Pro_{RR4} and Pro_{NSP2}:*GUS* patterns in nodule primordia (Figure 2D). Pro_{NSP2} activity was abolished when the three RRBSs identified were mutagenized, similarly to a Pro_{RR4} lacking the four RRBSs, suggesting that *NSP2* expression in nodules depends on these *cis*-elements.

Overall, these results indicate that *RR4* and *NSP2* are direct targets of the RR1-dependent cytokinin signaling pathway and that RRBS *cis*-elements are crucial to regulate their expression in response to cytokinins and during early nodule development.

The *MIR171 h* Gene Has an Opposite Expression Pattern to Its *NSP2* Target in Response to Cytokinins

In contrast with *RR4*, the *NSP2* expression pattern in response to cytokinins is very dynamic, with a transient induction followed by a rapid downregulation (Plet et al., 2011) (Figure 3A). Recently, a specific isoform of the miR171 microRNA (miRNA) was shown to cleave *NSP2* transcripts efficiently, suggesting a posttranscriptional regulation of this TF (Devers et al., 2011). To explore whether the dynamic regulation of *NSP2* in response to cytokinins could be linked to miR171 h, we analyzed its expression after a short-term cytokinin treatment. The *MIR171 h* precursor was continuously induced after 1- and 3-h treatments with 10^{-7} M of BAP, depending on the CRE1 pathway (Figure 3A), and displayed an opposite trend to *NSP2* expression 3 h after cytokinin application. Accordingly, a CRE1-dependent accumulation of mature miR171 h was observed in response to a 3-h treatment with 10^{-7} M of BAP (Figures 3A and 3B). Although *MIRNA* genes were not present on microarrays and therefore could not be considered in the bioinformatic screen, a manual inspection of the *MIR171 h* promoter revealed the presence of a RRBS core sequence in the proximal region of the promoter as well as an additional RRBS core–like sequence (Figure 3C), indicating that expression of this miRNA isoform may also be directly regulated by cytokinin. These results suggest that cytokinin regulation of *NSP2* is posttranscriptionally mediated by miR171 h.

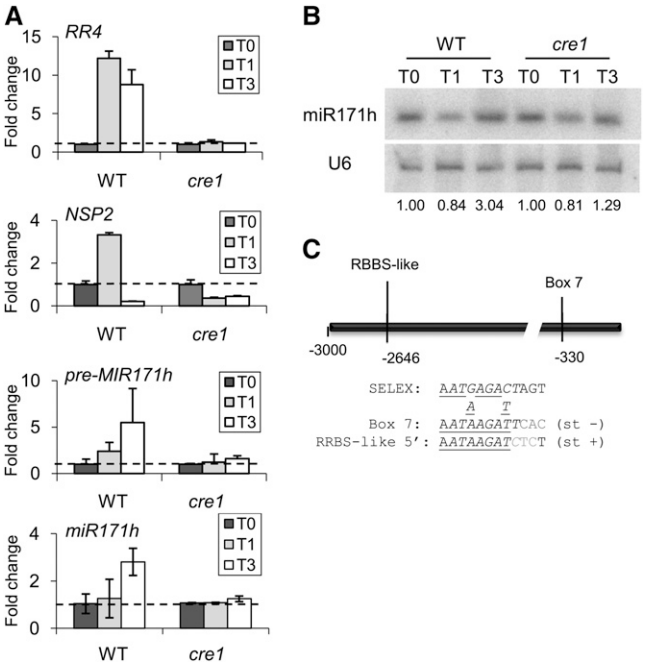

Figure 3. Cytokinins Regulate the miR171 h miRNA Targeting *NSP2*.

(A) Real-time RT-PCR analysis of *RR4*, *NSP2*, *MIR171 h* precursor (*pre-MIR171 h*), and mature *miR171 h* expression in roots of the wild type (WT) or of a *CRE1* cytokinin receptor mutant (*cre1-1*) treated for 1 or 3 h with 10^{-7} M of BAP. Error bars represent SD of two technical replicates, and one representative biological replicate out of four is shown ($n > 10$ independent transgenic roots/condition).

(B) RNA gel blot analysis to detect miR171 h mature small RNA in response to 10^{-7} M of BAP for 1 or 3 h in the wild type or the *cre1* mutant. The U6 RNA was used as a loading control, and calculated ratios normalized against the nontreated condition are indicated below the blots ($n > 10$ independent transgenic roots/condition).

(C) Schematic diagram of the *MIR171 h* promoter. A RRBS *cis*-element (box 7) is shown as well as an additional RRBS-like box (box 7 out of the 8-bp SELEX-core consensus). Alignment to the major SELEX consensus is shown below the promoter diagram. Gray indicates nonconserved nucleotides, underlined indicates conserved nucleotides between all boxes of each promoter, italics indicates 8-bp RRBS core, and st + or st − indicates DNA strand of sequences shown.

The bHLH476 TF Is a Direct Target of the CRE1 Pathway Positively Acting in Nodulation

To identify new cytokinin primary target genes potentially acting in nodulation, we then tested whether cytokinin regulation of selected genes (shown in Table 1) was impaired in the *cre1-1* mutant, which is essential for nodule organogenesis (Plet et al., 2011). In addition to *RR4* and *NSP2* genes, only transcripts encoding a bHLH TF (bHLH476) and a CKX (CKX1) were identified as CRE1-dependent (Figure 4A). The *bHLH476* and *CKX1* genes both contained a box 5 sequence, as in the case of *NSP2*, and an additional RRBS core variant (boxes 7 or 6, respectively; Figure 4B). ChIP-qPCR revealed that these two promoters were recognized in vivo by RR1 in *M. truncatula* roots (Figure 4C).

To determine the role of these genes in nodulation, *bHLH476* and *CKX1* expression was first analyzed using in situ hybridization. Whereas the expression level of the bHLH TF was beyond the detection threshold (in accord with the low expression levels detected using real-time RT-PCR; ~29 to 30 cycles), the *CKX1* gene was expressed in the different nodule zones (apical meristem, rhizobial infection/cell elongation zone, and nitrogen fixing zone; see Supplemental Figure 5 online). We then generated transgenic roots expressing RNAi constructs to silence these genes and tested their ability to nodulate under greenhouse optimal conditions. Only *bHLH476* RNAi roots revealed a significant decrease in nodule number and density (Figure 5A; see Supplemental Figure 6A online), despite the fact that a similar level of downregulation was obtained for both transcripts with the respective RNAi constructs (Figure 5B) and that no close homolog of this TF could be detected as expressed in roots and nodules. This phenotype was further confirmed in vitro at an earlier nodulation stage and by using a second independent RNAi

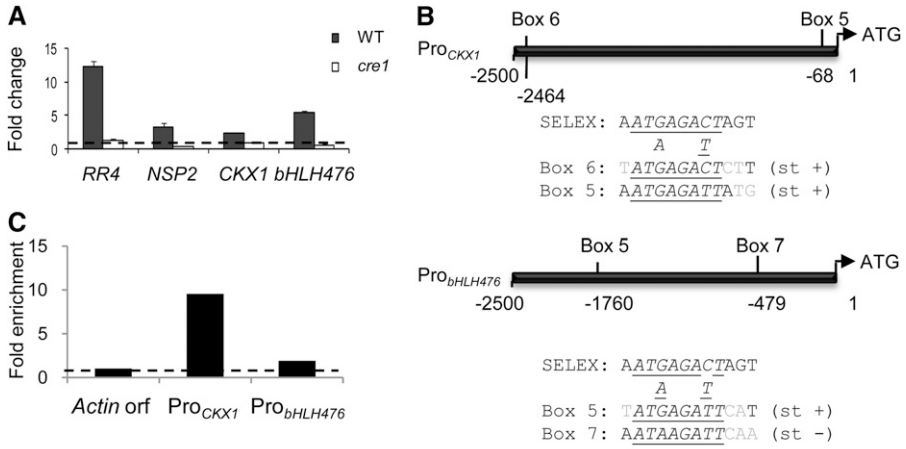

Figure 4. CRE1-Dependent Regulation of Primary Cytokinin Response Genes.

(A) Real-time RT-PCR analysis of selected candidate cytokinin primary response genes in roots of the wild type (WT) or of a *CRE1* cytokinin receptor mutant (*cre1-1*) treated for 1 h with 10^{-7} M of BAP. Genes tested are *RR4*, *NSP2*, *CKX1*, and *bHLH476*. The nontreated condition was set to 1 (dotted line) to visualize FCs. Error bars represent SD of two technical replicates, and one representative biological replicate out of four is shown ($n > 10$ independent transgenic roots/condition).

(B) Schematic diagram of the *CKX1* and *bHLH476* promoters. The different RRBS *cis*-elements variants (boxes 5 to 7) are indicated. Alignment to the major SELEX consensus is shown below each promoter diagram. Gray indicates nonconserved nucleotides, underlined indicates conserved nucleotides between all boxes of each promoter, italics indicates 8-bp RRBS core, and st + or st − indicates DNA strand of sequences shown.

(C) ChIP-qPCR of RR1 binding to *CKX1* and *bHLH476* promoters. *Actin11* ORF was used as a negative control, and IP values were normalized for each gene against the input genomic DNA. Ratios with *Actin11* were calculated to visualize RR1 binding fold enrichment ($n > 30$ independent transgenic roots/construct).

construct downregulating *bHLH476* expression (Figure 5C). In addition, a *Tnt1* insertional mutant predicted to generate a protein truncated in the middle of the bHLH domain (see Supplemental Figure 7 online) also showed a significantly reduced nodulation efficiency (Figure 5D; see Supplemental Figure 6B online). Microscopic analysis of *bhlh476* mutant roots infected with a *S. meliloti* strain expressing a Pro_{HemA}:*LACZ* reporter did not reveal any detectable defect in root hairs or infection thread progression (see Supplemental Figure 8 online). Hence, we identified a new bHLH TF as a direct target of the CRE1-dependent cytokinin signaling pathway positively regulating nodulation.

DISCUSSION

In this study, we have identified primary targets of a cytokinin-related RR using a transcriptomic analysis focused on *M. truncatula* root apices. Most previous studies aiming to assess transcriptome changes in response to cytokinins were performed in whole seedlings, and to our knowledge, such targeted analysis in roots had not been previously done in any plant. The most significantly enriched functional pathways regulated by cytokinins in *Medicago* roots were linked to GAs and flavonoids. Previous transcriptomic analyses in *Arabidopsis* revealed a connection with GA metabolism and response. Indeed, two GA biosynthesis genes (a GA20 oxidase gene and the 3β-hydroxylase gene *GA4*) were shown to be rapidly downregulated by cytokinins, whereas two genes encoding negative regulators of GA signal transduction (*GAI* and *RGA*) were upregulated (Brenner et al., 2005; Kiba et al., 2005). Our analysis further suggests that in *M. truncatula* root apices, several genes encoding GA-related oxidases and β-hydroxylases are upregulated after a short-term cytokinin treatment. GAs and cytokinins were shown to have an antagonistic action in *Arabidopsis* shoot and root apical meristems (Greenboim-Wainberg et al., 2005; Alabadí et al., 2009). In addition, GA regulates root growth in *Arabidopsis* as well as nodule formation in legumes (Ferguson et al., 2005; Greenboim-Wainberg et al., 2005; Achard et al., 2009; Maekawa et al., 2009; Ubeda-Tomás et al., 2009). By contrast, connections between cytokinin action and flavonoid metabolism are poorly documented. In legumes, spatial expression of a gene encoding chalcone synthase is modulated by cytokinins in white clover (*Trifolium repens*) roots (Mathesius et al., 2000). Our transcriptomic data revealed that many genes related to metabolic pathways leading to the biosynthesis of different types of flavonoids were upregulated in *Medicago* roots after a short-term cytokinin application, including 10 genes linked to isoflavonoid pathways, four linked to chalcone/flavone pathways, three linked to flavanones, and three linked to flavonols (based on the $P < 0.05$ threshold). This result strongly points to a role of cytokinins in activating flavonoid pathways in roots, which may not have been previously observed in *Arabidopsis*, either because whole seedlings were used or, alternatively, because this cross-talk may be legume-specific. Indeed, flavonoids have a critical role in early stages of the legume symbiotic interaction with rhizobia in relation to the activation of bacterial Nod factor production and to the initiation of nodule organogenesis through the regulation of polar auxin transport (Wasson et al., 2006; Oldroyd and Downie, 2008).

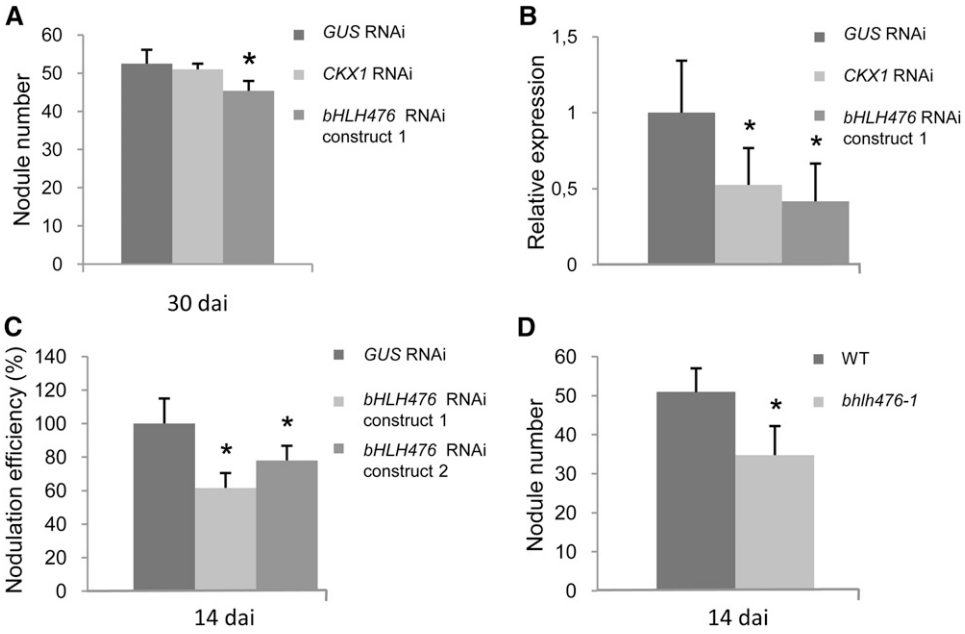

Figure 5. The bHLH476 Cytokinin Primary Response Transcription Factor Positively Regulates Symbiotic Nodulation.

(A) Quantification of the number of nodules formed under greenhouse conditions 30 DAI with *S. meliloti* on roots expressing RNAi constructs targeting *CKX1*, *bHLH476*, or GUS (as control), respectively.

(B) Real-time RT-PCR analysis of *CKX1* and *bHLH476* expression in roots expressing RNAi constructs targeting each gene or GUS (as control), respectively. The GUS RNAi control was set to 1 (dotted line). Error bars represent SD ($n = 5$ independent transgenic roots/construct), and a Kruskal-Wallis test was performed to assess significant differences ($\alpha < 0.05$).

(C) Quantification of the nodulation efficiency under in vitro conditions (14 DAI) of roots expressing RNAi constructs targeting *bHLH476* (two independent RNAi constructs) or GUS (as control), respectively.

(D) Quantification of the number of nodules formed under greenhouse conditions (14 DAI) on roots of a *Tnt1* insertional mutant affecting the *bHLH476* gene. WT, wild type.

In [**(A)**, **(C)**, and **(D)**], error bars represent confidence interval ($\alpha = 0.05$; $n > 30$ independent transgenic roots/genotype), and a Kruskal-Wallis **(A)** or Mann-Whitney [**(C)** and **(D)**] test was performed to assess significant differences ($\alpha < 0.05$).

Regarding genes encoding TFs, a significant enrichment for bHLH (discussed below) and AP2/ERF families was found. Previous transcriptomic analyses in *Arabidopsis* seedlings revealed that, in addition to the CRF subfamily, a few *Arabidopsis* AP2/ERF TFs were upregulated by cytokinins (Hoth et al., 2003; Rashotte et al., 2003; Brenner et al., 2005; Kiba et al., 2005). However, these genes are not closely related to the ones identified in *Medicago* roots. This result may indicate that legumes show differential regulation of TF subfamilies in response to cytokinins. In addition, the CRF requirement in cytokinin signaling may be different between seedlings and root apices.

The main goal of this study was to identify a set of cytokinin-regulated genes that could be direct primary targets of RR TFs acting in legume roots and nodules. Among several others, we selected the *RR* gene having the highest expression level in roots and nodules (Gonzalez-Rizzo et al., 2006; *M. truncatula* Gene Expression Atlas [http://mtgea.noble.org/v2/]). In *Medicago* roots, *RR1* silencing using two different RNAi constructs targeting a specific or a conserved region (Mt RR1-MYB domain RNAi) and Mt *RR1* overexpression did not reveal any significant cytokinin-sensitivity phenotype (Gonzalez-Rizzo et al., 2006; see Supplemental Figure 2 online). As observed in *Arabidopsis*, functional redundancy and compensation effects between different *RR* genes are likely to prevent the detection of cytokinin-sensitivity phenotypes (Mason et al., 2005). To circumvent these limitations, we ectopically expressed Mt *RR1* in *Arabidopsis*. The altered root cytokinin sensitivity observed suggests that Mt RR1 is involved in cytokinin signaling, even though, in contrast with the positive role of Type-B RRs described in *Arabidopsis* (Mason et al., 2005; Ishida et al., 2008), reduced cytokinin sensitivity was observed (see Supplemental Figure 2 online). This may be because of the ectopic expression in a heterologous context or alternatively may reveal a noncanonical function. Interestingly, a study analyzing the role of Type A *RR* genes showing opposite regulations in response to rhizobial Nod factors suggested their paradoxical role in *M. truncatula* root and nodule development. An RNAi construct targeting these RRs indeed negatively affected both lateral root and nodule formation (Op den Camp et al., 2011), in contrast with other studies affecting either *CKX* gene expression in *Lotus japonicus* or Mt *CRE1* (Lohar et al., 2004; Gonzalez-Rizzo et al., 2006), which revealed opposite functions of cytokinins in these organogeneses. Overall, these results suggest diverging roles for different members of either Type-B or Type-A RR families in nodulation. Further work is required to determine in each family which individual RRs act downstream of the CRE1 pathway to

regulate, either positively or negatively, cytokinin response and nodule organogenesis.

In contrast with the short 5-bp–consensus RR binding sequence identified in *Arabidopsis*, our study identified a larger 12-bp *cis*-element consensus, which allowed the application of reliable bioinformatic searches for candidate cytokinin primary response genes. Based on a criteria of RRBS *cis*-element enrichment in promoters of cytokinin-regulated genes, we retrieved the expected Type-A RR Mt *RR4* and two homologs of genes previously reported in *Arabidopsis* (*CKX1* and *GST*; Taniguchi et al., 2007), indicating a certain conservation between these two plant species. Interestingly, both RR4 and CKX1 are proposed to mediate negative feedback on the cytokinin pathway by affecting signaling or the hormonal pool, respectively. A systematic search for homologs of previously reported *Arabidopsis* cytokinin primary response genes (Taniguchi et al., 2007) in the transcriptomic data revealed six additional homologs containing at least one RRBS 8-bp core sequence in their promoter and upregulated by cytokinins in *Medicago* root apices (see Supplemental Data Set 2 online). Among those, an AUX-IAA protein closely related to SHY2/IAA3 acting in *Arabidopsis* root meristems (Dello Ioio et al., 2008) contained three RRBS core sequences. The higher RR1 binding efficiency to box 2 than to box 5 (Figure 2B) suggests that the *cis*-element is better recognized when a C is at the eighth position of the AATGAGA(T/C)TAGT sequence. Further work is therefore needed to decipher precisely which RR binds to each RRBS variant and to determine the relevance of the number and location of RRBS *cis*-element combinations, because tandem organizations of RRBS were retrieved in the two promoters analyzed.

Among the candidate cytokinin primary response genes identified, *NSP2* encodes one of the most upstream TFs previously described as acting in early nodulation, both in cortical and epidermal cells (Oldroyd and Downie, 2008; Madsen et al., 2010; Figure 6). RRBS *cis*-elements present in the *NSP2* promoter are required in planta both for cytokinin regulation and expression in nodule primordia. This strongly suggests that a direct regulation of *NSP2* expression by the CRE1-dependent signaling pathway occurs during early nodule organogenesis, where both CRE1 and NSP2 act (Kaló et al., 2005; Plet et al., 2011). Unfortunately, we were not able to complement the *nsp2* mutant using a 2.5-kb Pro_{NSP2}:*NSP2* construct, preventing us from testing the functional relevance of cytokinin regulation through the RRBS in nodulation. In addition, our results indicate that the tight and dynamic regulation of *NSP2* expression (upregulated after a 1-h cytokinin treatment and repressed at later time points; Gonzalez-Rizzo et al., 2006; Maekawa et al., 2009; Plet et al., 2011) may involve posttranscriptional regulation by the miR171 h miRNA. Whereas several miRNAs were shown to be regulated by auxin and/or to target the auxin signaling pathway, this is the first cytokinin-regulated miRNA (Liu and Chen, 2009). Other TFs linked to nodulation and acting downstream of the CRE1 cytokinin receptor are Mt ERF Required for Nodulation1 (ERN1; Middleton et al., 2007) and Nodule Inception (NIN; Schauser et al., 1999; Madsen et al., 2010; Plet et al., 2011). Despite the fact that no enrichment for RRBS *cis*-elements was found in these promoters, certain cores similar to the SELEX consensus could be detected (see Supplemental Figure 9 online). We can speculate that cytokinin regulation of *NIN* and *ERN1* may be also dependent on Type-B RRs.

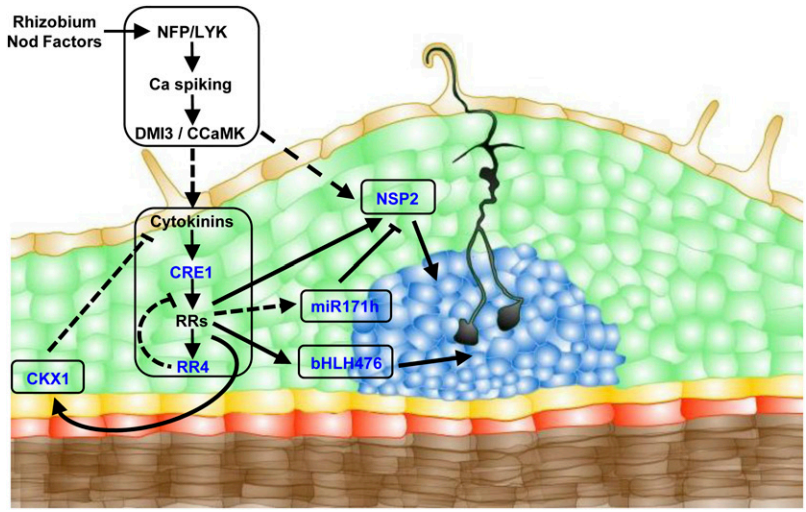

Figure 6. Downstream Cytokinin Signaling Events in Symbiotic Nodulation.

Schematic representation of a *M. truncatula* symbiotic nodule primordium, including selected known components of the *Rhizobium* Nod factor signaling pathway (Nod Factor Perception/Lys-M Kinase receptor [NFP/LYK], Does Not Make Infections/Calcium Calmodulin Protein Kinase [DMI3/CCaMK], Nod factor Signaling Pathway2 [NSP2]) and of the cytokinin signaling pathway (Cytokinin Response1 [CRE1], Response Regulators [RRs]). New genes identified in this study as acting downstream of the CRE1/RR cytokinin pathway are also indicated: the miR171 h isoform targeting NSP2 and the new direct cytokinin targets bHLH476 and CKX1. Proven interactions are indicated by full lines, and putative interactions by dotted lines.
Orange indicates epidermis, green indicates cortex, yellow indicates endodermis, red indicates pericycle, brown indicates stele, and blue indicates nodule primordium.

Our study additionally identified a new regulatory gene acting directly downstream of the CRE1 cytokinin pathway and positively regulating symbiotic nodulation: the bHLH476 TF (Figure 6). Previous transcriptomic analyses performed in *Arabidopsis* seedlings revealed that at least five bHLH TFs were rapidly upregulated by cytokinins (At2g18300, At2g22770, At4g25410, At5g50915, At5g65640; Hoth et al., 2003; Brenner et al., 2005; Kiba et al., 2005; Lee et al., 2007). Apart from its bHLH DNA BD, the *Medicago* bHLH476 TF is not closely related to any of these genes or to any of the bHLH TFs functionally characterized in legumes (Figure 7). Accordingly, in contrast with *root hair less1/slippery* mutants (*rhl1*; Karas et al., 2009), we did not detect any root hair phenotype in *bhlh476* mutants or in plants carrying RNAi constructs targeting this gene. Furthermore, infection thread progression was similar to the wild type. Future experiments, including overexpression studies, will help to determine whether bHLH476 is involved in nodule organogenesis. Hence, the bHLH476 cytokinin primary target may have been specifically recruited in legume roots at the convergence of cytokinin and nodulation cues.

Overall, using a combination of transcriptomic, biochemical, and molecular approaches, we unveiled new transcriptional and posttranscriptional networks acting in symbiotic nodule organogenesis downstream of the CRE1 signaling pathway. Among the novel primary targets of cytokinin action identified, the NSP2 and bHLH476 TFs were linked to nodulation, suggesting their

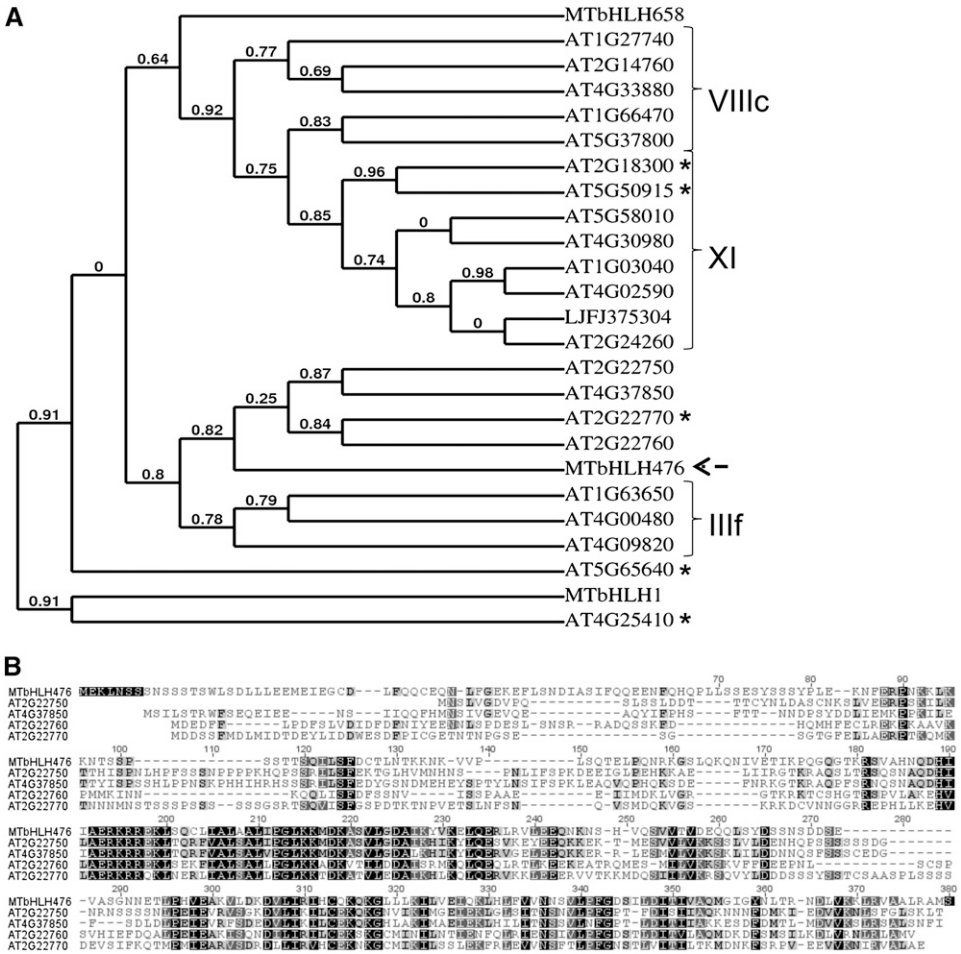

Figure 7. bHLH476 Is Not Closely Related to any Known Cytokinin Response and Nodulation Genes.

(A) Phylogenetic tree of bHLH TFs functionally characterized in legumes (LjFJ375304/ROOTHAIRLESS1 [RHL1]/SLIPPERY [Karas et al., 2009]; MtbHLH1 [Godiard et al., 2011]; MtbHLH658 [Zahaf et al., 2012]), previously linked to *Arabidopsis* cytokinin response, or related to MtbHLH476 (arrow). Complete proteins were aligned at http://www.phylogeny.fr/ using MUSCLE 3.7, PhyML 3.0 phylogenetic analysis, and TreeDyn (PHYLIP package) displays. Numbers indicate the branch support values as the likelihood a posteriori. Asterisks indicate the cytokinin-responsive *bHLH* genes identified in *Arabidopsis*. Groups and subgroups of bHLH proteins are indicated at the right, according to Karas et al. (2009). Sequences are available from The Arabidopsis Information Resource (http://www.*Arabidopsis*.org/) and from GenBank (http://www.ncbi.nlm.nih.gov/) or TIGR (http://compbio.dfci.harvard.edu/tgi/plant.html) databases for legume species. The alignment is available in Supplemental Data Set 4 online.

(B) Protein alignment (using ClustalW) of MtbHLH476 with its closer *Arabidopsis* homologs: At2g22750, At2g22760, At2g22770, and At4g37850. Black boxes indicate identity between the five sequences, and gray boxes indicate identity in at least three sequences.

recruitment in legumes into specific symbiotic functions. The identification of extended RRBS *cis*-elements also opens global perspectives to develop artificial reporters to monitor specifically cytokinin responses in plants.

METHODS

Biological Material

Medicago truncatula cv Jemalong A17 wild type and the *cre1-1* mutant allele (Plet et al., 2011) were used in this study, as well as *Arabidopsis thaliana* (Colombia-0 ecotype). In addition, a *M. truncatula* mutant derived from the T00007H line of the Jemalong A17 *Tnt1* collection was identified as having an insertion located at nucleotide 664 (from the ATG) in the *bHLH476* gene (*bhlh476-1* allele; see Supplemental Figure 7 and Supplemental Data Set 3 online for genotyping primers). Seeds were sterilized for 20 min in bleach (12% [v/v] sodium hypochlorite). After washing with sterilized water, seeds were sown on 1% agar plates and stored for 2 d at 4°C before incubating overnight at 24°C in the dark to ensure uniform germination. Germinated seedlings were transferred to square plates containing appropriate medium (see below) and grown vertically in chambers at 24°C under long-day conditions (16 h light at 150 μE light intensity/8 h dark).

For nodulation experiments, germinated seeds were grown in vitro on low-nitrogen medium (Fahraeus medium without nitrogen; Truchet et al., 1985). Roots were inoculated with 10 mL of the *Sinorhizobium meliloti* strain 1021 suspension (OD_{600} = 0.05) per plate for 1 h. A derivative *S. meliloti* strain 2011 (GMI6390, pMH682) (GMI6526; Ardourel et al., 1994) carrying the pXLGD4 plasmid containing a Pro_{HemA}:*LACZ* transcriptional fusion was additionally used.

Hormone Treatments

Fifteen germinated seedlings were placed on a grid in a Magenta box with 30 mL of low-nitrogen liquid medium ("i"; Blondon, 1964) and grown in a shaking incubator (125 rpm) at 24°C under long-day conditions (16 h light/8 h dark). After 5 d, seedlings were treated with or without 10^{-7} M of BAP (Sigma-Aldrich) and maintained under the same growth conditions for various incubation times (0, 1, and 3 h). In parallel, mock experiments were performed, which consisted of collecting nontreated roots across the kinetic (0, 1, and 3 h). No significant variation in expression of any of the genes tested was observed in three independent replicates. Roots were collected at the indicated time points and immediately frozen in liquid nitrogen for RNA extraction. In all cases, four independent biological experiments were performed ($n > 10$).

Cloning, Expression, and Purification of Recombinant Protein

A region of Mt RR1 (JQ647414, GenBank database [http://www.ncbi.nlm.nih.gov]) containing the DNA BD coding sequence (RR1 BD) was selected (residues 69 to 229; see Supplemental Figure 10 online), PCR-amplified, and inserted in frame into the *Bam*HI and *Eco*RI sites of the expression vector pGEX-3X (Smith and Johnson, 1988) to generate a GST fusion. Amplifications were performed using oligonucleotides RR1-BD1 (5′-CGCGGATCCCAATTTCCCACGGTGCCC-3′) and RR1-BD2 (5′-CACGAATTCGTCTGGATATCCTTGCTG-3′), where sequences underlined correspond to *Eco*R1 and *Bam*H1 restriction sites, respectively. *Escherichia coli* cells, strain JM109 (GE Healthcare), were transformed with the Mt RR1 BD pGEX-3X fusions and then grown and induced for 3 h as described in Palena et al. (1998). However, the incubation after induction with isopropyl-β-D-1-thiogalactopyranoside (Sigma-Aldrich) was performed at 28°C. Recombinant proteins were purified using the GST-tag (GE Healthcare; Kaelin et al., 1992), and stored at −80°C in 5% glycerol.

PCR-Assisted Binding Site Selection

To select DNA molecules specifically bound by the purified recombinant RR1 BD, the random oligonucleotide selection technique (SELEX; Oliphant et al., 1989) was applied, using procedures described by Blackwell and Weintraub (1990). A ^{32}P-labeled (30,000 cpm) 51-mer double-stranded oligonucleotide containing a 12-bp random central core [5′-GATGAAGCTTCCTGGACAAT(12N)GCAGTCACTGAAGAATTCT-3′] was incubated with purified GST-Mt RR1 BD as described above. Bound DNA molecules were separated by EMSA and eluted from gel slices with 0.5 mL of 0.5 M NH_4Ac, 10 mM $MgCl_2$, 1 mM EDTA, and 0.1% (w/v) SDS. The selected DNA molecules were amplified using oligonucleotides R1 (5′-GATGAAGCTTCCTGGACAAT-3′) and R2 (5′-CAGAATTCTTCAGTGACTGC-3′). Amplification reactions were performed as follows: 18 cycles of 1 min at 94°C, 1 min at 53°C, and 1 min at 72°C. The number of cycles was decreased to 12 after the fourth round. After purification through polyacrylamide gels, the amplified molecules were subjected to new cycles of binding, elution, and amplification. Enrichment in sequences bound specifically by Mt RR1 BD was monitored by binding and competition analysis in EMSA. After seven rounds of selection, the population of oligonucleotides was cloned into the pCR 2.1-TOPO vector (Invitrogen). Thirty-eight randomly picked clones were sequenced.

DNA Binding Assays

For EMSA performed with synthetic probes, aliquots of the purified proteins were incubated with double-stranded DNA (0.3 to 0.6 ng, 30,000 cpm, labeled with [α-^{32}P] dATP by filling in the 3′-ends using the Klenow fragment of DNA polymerase) generated by hybridization of the complementary synthetic oligonucleotides 5′-AATTCACATATAATGAGACTAGTTGAG-3′ and 5′-GATCCTCAACTAGTCTCATTATATGTG-3′ or derivatives with modifications within the binding sequence (underlined) as described in the Results and Supplemental Data Set 3 online. Binding reactions (20 μL) containing 20 mM of HEPES (pH 7.5), 50 mM of KCl, 2 mM of $MgCl_2$, 0.5 mM of EDTA, 1.0 mM of DTT, 0.5% Triton X-100, 22 ng/μL of BSA, 1 μg of poly(dI-dC), and 10% glycerol were incubated for 15 min at room temperature, supplemented with 2.5% Ficoll, and immediately loaded onto a running gel (5% acrylamide, 0.08% bis-acrylamide in 0.5× TBE plus 2.5% glycerol; 1× TBE is 90 mM of Tris-borate, pH 8.3, and 2 mM of EDTA). The gel was run in 0.5× TBE at 20 mA for 2 h and dried before autoradiography. When competition assays were performed, 100-fold unlabeled double-stranded oligonucleotides were included in the binding reaction mix and incubated for 10 min before the addition of the selected labeled oligonucleotide. For competition EMSAs, fresh DTT was added to avoid the formation of the double band typically caused by GST oligomerization.

In Situ Hybridization, Real-time RT-PCR, ChIP, and RNA Gel Blot Analysis

In situ hybridizations were performed as described in Bustos-Sanmamed et al. (2012) on nodules 21 d after *S. meliloti* inoculation using an Intavis InsituPro automat (http://www.intavis.com/en/). Antisense RNA probes corresponding to Mt *bHLH476* and Mt *CKX1* were generated as well as an Mt *CKX1* sense probe as negative control (primers shown in Supplemental Data Set 3 online).

For real-time RT-PCR, total RNA was extracted from frozen roots using the RNeasy plant mini kit (Qiagen). First-strand cDNA was synthesized from 1.5 μg of total RNA using the Superscript II First-Strand Synthesis System (Invitrogen). Primer design was performed using Primer3 software (http://frodo.wi.mit.edu/cgi-bin/primer3/). Primer combinations showing a minimum amplification efficiency of 90% were used in real-time RT-PCR experiments (see Supplemental Data Set 3 online). Real-time RT-PCR reactions were performed using the LightCycler480 SYBR Green I Master

Kit on a LightCycler480 apparatus according to manufacturer's instructions (Roche). Cycling conditions were as follows: 95°C for 10 min, 40 cycles at 95°C for 5 s, 60°C for 5 s, and 72°C for 15 s. PCR amplification specificity was verified using a dissociation curve (55 to 95°C), as well as systematic sequencing of PCR amplicons. A negative control without cDNA template was always included for each primer combination. Technical replicates (on two independent syntheses of cDNA derived from the same RNA sample) and four independent biological experiments ($n > 10$) were performed in all cases. Ratios were done with constitutive controls for gene expression to normalize the data between different biological conditions. Mt *ACTIN*, Mt *RBP1*, and Mt *H3L* were selected using Genorm software (http://medgen.ugent.be/~jvdesomp/genorm/; Vandesompele et al., 2002) as reference genes for experiments involving hormonal treatments in wild-type and *cre1* mutant roots (primers shown in Supplemental Data Set 3 online). Mt *RBP1* was chosen to calculate ratios, and the value of the experimental control condition was set to 1 as a reference to determine relative expression or induction factors.

For ChIP experiments, roots expressing the Mt RR1-hemagglutinin (HA) fusion were used (see below). Purification of root nuclei expressing this construct or an empty vector and HA immunoprecipitation (IP) were done as in Ariel et al. (2010). The different promoters analyzed, as well as the *Actin11* open reading frame (ORF, used as negative control, same primers as for RT-PCR), were amplified by real-time PCR from the input genomic DNA (i.e., before IP) and after IP (primers indicated in Supplemental Data Set 3 online; cycling conditions as for RT-PCR). For each gene, the input data were used to normalize results obtained from the IP extracts and the *Actin11* ORF as a calibrator. Two independent biological experiments (each based on a pool of $n > 30$ independent transgenic roots per construct) were performed.

Small RNA gel blots were performed following the protocol described in Boualem et al. (2006), using the 5′-GAGTGATATTGATTCGGCTCG-3′ probe to detect the specific miR171 h isoform. The U6 RNA, used as loading control, was detected with the following probe: 5′-GCAGGGGCCATGCTAATCTTCTCTGTATCGT-3′. The expression profile of the miR171 h isoform was assayed in parallel using stem–loop real-time RT-PCR, as described by Varkonyi-Gasic et al. (2007), using the primer miR171 h-RT 5′-GTCGTATCCAGTGCAGGGTCCGAGGTATTCGCACTGGATACGACGAGTGA-3′ and primers indicated in Supplemental Data Set 3 online for subsequent real-time PCR.

Hybridization of Microarrays, Data Processing, Statistical Analyses, MapMan Display, and Bioinformatic Workflow

For microarray analysis of the root apices' response to cytokinins, germinated seedlings were transferred to perlite:sand (3:1) pots without bottoms on a grid and were grown until roots passed through the grid (as described in Gruber et al., 2009). The liquid plant growth media SN/2 (Soluplant 18.6.26; Duclos International) in which the emerging root apices were immersed was replaced by fresh medium with or without 10^{-7} M of BAP for 1 h. Four biological replicates for each condition (treated and nontreated) were performed (using at least nine plants per replicate). Root apices (1 cm) were harvested, immediately frozen in liquid nitrogen, and stored at −80°C for RNA extraction.

RNAs were extracted as described above for RT-PCR. RNA quality was checked using an Agilent 2100 Bioanalyzer (Agilent). A total of 2 μg of each sample were used to synthesize Cy5/Cy3-labeled cDNA using the Amino Allyl Message Amp II aRNA Amplification kit (Ambion) according to the manufacturer's instructions. Samples were balanced with respect to dyes: for each experimental condition, the four independent biological samples were labeled with both the Cy5 and Cy3 dyes. This ensures that the effects of interest are not biased by genes interacting with dyes. Cy5/Cy3-labeled cDNA were hybridized with the 70-mer Mt16K+ oligonucleotide microarrays (http://www.ebi.ac.uk/microarray-as/ae/; accession number A-MEXP-138, ArrayExpress database) for 16 h at 60°C in a rotating oven (6 rpm) using an Agilent hybridization chamber system. The hybridized slides were washed in 1× SSC and 0.2% SDS for 10 min at 50°C, 0.1× SSC for 10 min at room temperature, 0.05× SSC for 5 min at room temperature twice, and water at room temperature for 1 min. All washes were done in the dark with gentle agitation.

Microarray slides were scanned with a GenePix two-laser scanner (Axon Instruments), and the resulting images were analyzed with the GenePix 6.0 software (Molecular Devices). Data transformations and normalization, performed with the MAnGO R script (version 1.0; Marisa et al. 2007), consisted of a local background correction, omitting flagged spots, and then an intensity-dependent print-tip loess normalization and a scale between array normalization (Yang et al. 2002). Minimum Information About a Microarray Experiment (MIAME)–compliant data were deposited in the ArrayExpress database (http://www.ebi.ac.uk/microarray-as/ae/) under the accession number E-MEXP-1442. Differential analysis was based on an empirical Bayes moderated *t* test adjusted with the false discovery rate (Benjamini and Hochberg, 1995) multiple test correction. Differentially expressed genes were selected based on adjusted P-values, and a background threshold was defined based on a mean intensity of the two channels (A-mean) > 7 on a $\log_2$ scale (threshold based on negative controls available in the microarray).

Data were visualized using the MapMan software (http://gabi.rzpd.de/projects/MapMan/; Thimm et al., 2004; Tellström et al., 2007), following instructions provided on the website. To predict functional categories showing an enrichment in the differentially regulated genes, we used | fold change (FC) | > 1.5 and adjusted $P < 0.001$ thresholds to maximize the relevance of the analysis. MapMan bins were used to perform a Fisher's exact test ($P > 0.05$), and categories with more than 10 elements and for which at least three were differentially regulated were retained. To scan promoter regions for the RRBS cores, the REMORA Workflow *GetAndScanPromoterRegionsFromAListOfMedicagoIDsToUniqueIDs* was used (http://www.legoo.org/; Carrere and Gouzy, 2006). Cytokinin-regulated genes were defined based on less stringent criteria (| FC | > 1.5 and adjusted $P < 0.05$) to allow the identification of the maximum number of promoter regions. The following parameters were set in the workflow: coverage used to define genomic regions corresponding to The Institute for Genomic Research (TIGR) tentative consensus (TC) accession numbers, 90%; promoter length, 2500 bp (defined based on our analysis of RRBS in the Mt *RR4* promoter; see Results). PatScan strings were based on box sequences indicated in Supplemental Data Set 2 online followed by [0,0,0], meaning that only perfect matches were allowed.

Cloning, Site-Directed Mutagenesis, and *Agrobacterium* spp Transformation

For Mt RR4 transcriptional fusion, a 3030-bp sequence upstream of the RR4 start codon was amplified by PCR using a Pfx polymerase (Invitrogen) and primers *RR4pro-F* and *RR4pro-R* (as described in Plet et al. [2011]) (see Supplemental Data Set 3 online). A 1133-bp proximal promoter region (referred to as Δbox) was also amplified with primers *prox-RR4-F* and *RR4pro-R* (see Supplemental Data Set 3 online). Pro_{RR4} box 2 was mutagenized using the QuikChange Site-Directed Mutagenesis Kit (Stratagene) using the primers *RR4-box2-F* and *RR4-box2-R* (see Supplemental Data Set 3 online).

For Mt NSP2 transcriptional fusion, a 2.5-kb sequence upstream of the *NSP2* ATG start codon was similarly amplified using primers *NSP2-pro-F* and *NSP2-pro-R* (see Supplemental Data Set 3 online). The region between −616 bp and −802 bp was replaced by a *Bam*H1 restriction site by PCR amplification (Δbox construct; primers *NSP2-del-F* and *NSP2-del-R*; see Supplemental Data Set 3 online) and subcloned in a pBluescript-SK− vector (Addgene).

The three RRBSs in the *NSP2* promoter were successively mutagenized using the QuikChange Site-Directed Mutagenesis Kit (Stratagene) to replace the GAGA central core by an ACTG sequence, leading

to the $Pro_{NSP2\text{-}3XMut}$ construct. This was achieved using the following primers for each box: mutB5-5′F/mut B5-5′R, mutB5-3′F/mut B5-3′R, and mut B6 F/mut B6 R (see Supplemental Data Set 3 online).

The different promoter constructs were finally cloned using Gateway technology from the pTopo-Entry vector (Invitrogen) into the pkGWFS7 vector (http://www.psb.ugent.be/gateway/index.php) carrying a *green fluorescent protein* (*GFP*)-*GUS* fusion downstream of the cloning recombination site.

The RNAi constructs targeting either the Mt RR1 conserved MYB domain (Mt RR1-MYB domain) or the Mt *bHLH476* gene were cloned in the pFRN vector (Gonzalez-Rizzo et al., 2006) using primers indicated in Supplemental Data Set 3 online. The pFRN GUS RNAi control is described in Gonzalez-Rizzo et al. (2006). The 35S-CaMV:RR1-HA construct was cloned in-frame with a C-terminal HA tag and was transferred into a pMF plant expression vector (Merchan et al., 2007; primers indicated in Supplemental Data Set 3 online). The empty vector, containing a 35S:GUS cassette, was used as control.

The resulting constructs were introduced into *Agrobacterium rhizogenes* ARqua1 (streptomycin-resistant derivative strain of A4T; Quandt et al., 1993) and were used for *M. truncatula* root transformation. The transgenic roots were obtained after kanamycin (25 mg/L) selection for 2 weeks as described by Boisson-Dernier et al. (2001). Composite plants were then transferred onto growth papers (Mega International) on Fahraeus medium without nitrogen (Truchet et al., 1985) for 4 to 6 d and were further used to test cytokinin or nodulation responses (as described before). In addition, the 35S-CaMV:RR1-HA construct was introduced in *Arabidopsis* ecotype Columbia-0 using the *A. tumefaciens* floral dipping method, and several independent transformed lines were selected on kanamycin (50 mg/L).

Fluorometric Assays, Histochemical Staining, and Microscopic Analyses

To analyze expression of the *GUS* reporter in response to a short-term cytokinin treatment, a fluorometric assay was performed to quantify the induction FC in response to BAP treatment. Composite plants generated as described above were transferred to Fahraeus liquid medium and grown for another 3 d. Plants were individually identified, a part of each root (~0.5 mg) was frozen in liquid nitrogen, and samples were stored at −80°C. After 2 d, the same plants were treated for 3 h with 10^{-7} M of BAP, and a new sample of each root was frozen with liquid nitrogen. Specific GUS activity in protein extracts was measured using the fluorogenic substrate 4-methylumbelliferyl β-D-glucuronide (Sigma-Aldrich) essentially as described by Welchen and Gonzalez (2005). Total protein extracts were prepared by grinding root tissues in extraction buffer (50 mM sodium phosphate, pH 7.0, 10 mM EDTA, 10 mM β-mercaptoethanol) containing 0.1% (w/v) SDS and 1% Triton X-100, followed by centrifugation at 13,000*g* for 10 min. GUS activity was measured with 1 mM of 4-methylumbelliferyl β-D-glucuronide and 20% methanol. The results were expressed as a ratio between the values obtained after and before the treatment for each individual root ($n > 20$).

To analyze expression of the GUS reporter during nodulation, composite plants were inoculated with the *S. meliloti* strain 1021 (as described before). Three independent biological experiments were performed ($n = 25$). Histochemical stainings were performed as previously described (Pichon et al., 1992); samples were incubated in darkness for up to 16 h at 37°C. Roots and nodules infected by the Pro_{HemA}*:LACZ* strain were used for β-galactosidase staining (overnight at 30°C), as described in Ardourel et al. (1994). In both cases, after staining, roots were observed 3 to 5 d after inoculation (DAI) with *S. meliloti* in bright field using a Nikon AZ100 microscope equipped with a DFC 300 camera.

Phylogenetic Analysis

The phylogenetic reconstruction was performed using the default parameters of the PHYLIP package (http://www.phylogeny.fr/). Sequences were aligned with MUSCLE (v3.7; Edgar, 2004) configured for highest accuracy (MUSCLE with default settings), and the Gblocks program (v0.91b) was used to eliminate poorly aligned positions and divergent regions. The alignment is available in Supplemental Data Set 4 online. The phylogenetic tree was reconstructed using the maximum likelihood method implemented in the PhyML program (v3.0 aLRT). The WAG substitution model was selected, assuming an estimated proportion of invariant sites (of 0.073) and four γ-distributed rate categories to account for rate heterogeneity across sites. The γ shape parameter was estimated directly from the data ($\gamma = 3.959$). Reliability for internal branch was assessed using the aLRT test (SH-Like). Graphical representation and editing of the phylogenetic tree were performed with TreeDyn (v198.3). Numbers indicate the branch support values as the likelihood a posteriori. Sequences are available from The Arabidopsis Information Resource (http://www.*Arabidopsis*.org/) and from GenBank (http://www.ncbi.nlm.nih.gov/) or TIGR (http://compbio.dfci.harvard.edu/tgi/plant.html) for legume species.

Accession Numbers

Sequence data from this article can be found in the Arabidopsis Genome Initiative or GenBank/EMBL databases under the following accession numbers: Mt RR1, JQ647414. The 70-mer Mt16K+ oligonucleotide microarrays are deposited in the ArrayExpress database (http://www.ebi.ac.uk/microarray-as/ae/) under accession number A-MEXP-138, and microarray experiment–compliant data of the transcriptomic experiment are deposited under the accession number E-MEXP-1442.

Supplemental Data

The following materials are available in the online version of this article.

Supplemental Figure 1. Metabolic Processes, Hormonal Pathways, and Large Enzymatic Families Regulated in Response to a Short-Term Cytokinin Treatment in Root Apices.

Supplemental Figure 2. Mt RR1 Overexpression in *Arabidopsis* Affect Root Sensitivity to Cytokinins.

Supplemental Figure 3. Raw Sequences Cloned after Seven Rounds of Binding Site Selection Using SELEX.

Supplemental Figure 4. Competition EMSA Comparing the in Vitro Binding Preference of GST-RR1 BD for Alternative RRBS.

Supplemental Figure 5. Expression Pattern of Mt *CKX1* in Nodules.

Supplemental Figure 6. Nodule Density of *bHLH476* RNAi Roots.

Supplemental Figure 7. Nucleotidic and Protein Sequence of the bHLH476 TF and Location of the *Tnt1* Insertion.

Supplemental Figure 8. Root Hair and *Rhizobium* Infection Phenotype of *bhlh476* Mutants.

Supplemental Figure 9. Schematic Diagrams of Promoter Regions of *ERN1* and *NIN* Cytokinin Nodulation-Related Genes.

Supplemental Figure 10. Protein Sequence of the Mt RR1 RR.

Supplemental Table 1. Differentially Expressed Functional Categories in Response to Cytokinins (10^{-7} M of BAP for 1 h) in Root Apices Based on MapMan Bins.

Supplemental Data Set 1. Detailed List of Differentially Expressed Genes in Response to Cytokinins (10^{-7} M of BAP for 1 h) in Root Apices.

Supplemental Data Set 2. Detailed List of Candidate Cytokinin-Regulated Genes with RRBS Boxes in Their Promoters.

Supplemental Data Set 3. List of Primers.

Supplemental Data Set 4. Text File of the Alignment Used to Generate the Phylogenetic Tree Shown in Figure 7.

ACKNOWLEDGMENTS

We thank Hervé Delacroix and Sandrine Imbeaud (Gif/Orsay DNA Micro-Array Platform, Centre National de la Recherche Scientifique, Gif-sur-Yvette, France) for statistical analyses of the microarray data, Marion Verdenaud (Laboratoire des Interactions Plantes Micro-organismes, Castanet-Tolosan, France) for her involvement in setting up the bioinformatic workflow, and Elena Carvajal (Tétraèdre, France) for artwork. We also thank the anonymous reviewers for their constructive comments. Microscopy was done on the Imagif platform (Centre National de la Recherche Scientifique, Gif-sur-Yvette, France). This project was done in the frame of the French Agence Nationale de la Recherche project LEGUROOT, which also funded M.B.-H. The *Tnt1* mutant collection was generated in the frame of the GRAIN LEGUME (GLIP-EEC-FP6) project. Work in Argentina was supported by Agencia Nacional de Promoción Científica y Tecnológica (PICT 2005 38103 and PICT 2007 37000/022). R.L.C. is a member of Consejo Nacional de Investigaciones Científicas y Técnicas, and F.A. was a fellow of the same institution. We thank the ECOS-Sud program A07B03, the Argentinean Ministry of Education, the French Embassy, and the Banco Santa Fe Foundation for providing short-term fellowships to F.A. J.P. was the recipient of a doctoral grant from the Ministère de la Recherche et de la Technologie (France), and S.B. was supported by a GRAIN LEGUME (GLIP-EEC-FP6) fellowship.

AUTHOR CONTRIBUTIONS

F.F. designed the research; F.A., M.B.-H., C.L., E.H., M.B., J.P., M.M, S.B., and R.L.C. performed research; S.C. and M.C. contributed new computational tools; F.A., M.B.-H., C.L., E.H., J.P., M.M, S.B., J.L.I., R.L.C., and F.F. analyzed data; F.A., M.B.-H., M.C., and F.F. wrote the article.

Received July 26, 2012; revised August 28, 2012; accepted September 10, 2012; published September 28, 2012.

REFERENCES

Achard, P., Gusti, A., Cheminant, S., Alioua, M., Dhondt, S., Coppens, F., Beemster, G.T., and Genschik, P. (2009). Gibberellin signaling controls cell proliferation rate in *Arabidopsis*. Curr. Biol. **19:** 1188–1193.

Alabadí, D., Blázquez, M.A., Carbonell, J., Ferrándiz, C., and Pérez-Amador, M.A. (2009). Instructive roles for hormones in plant development. Int. J. Dev. Biol. **53:** 1597–1608.

Ardourel, M., Demont, N., Debellé, F., Maillet, F., de Billy, F., Promé, J.C., Dénarié, J., and Truchet, G. (1994). *Rhizobium meliloti* lipooligosaccharide nodulation factors: Different structural requirements for bacterial entry into target root hair cells and induction of plant symbiotic developmental responses. Plant Cell **6:** 1357–1374.

Ariel, F., Diet, A., Verdenaud, M., Gruber, V., Frugier, F., Chan, R., and Crespi, M. (2010). Environmental regulation of lateral root emergence in *Medicago truncatula* requires the HD-Zip I transcription factor HB1. Plant Cell **22:** 2171–2183.

Benjamini, Y., and Hochberg, Y. (1995). Controlling the false discovery rate: A practical and powerful approach to multiple testing. J. R. Stat. Soc., B **57:** 289–300.

Blackwell, T.K., and Weintraub, H. (1990). Differences and similarities in DNA-binding preferences of MyoD and E2A protein complexes revealed by binding site selection. Science **250:** 1104–1110.

Blondon, F. (1964). Contribution à l'étude du développement de graminées fourragères: Ray-grass et dactyle. Rev. Gen. Bot. **71:** 293–381.

Boisson-Dernier, A., Chabaud, M., Garcia, F., Bécard, G., Rosenberg, C., and Barker, D.G. (2001). *Agrobacterium rhizogenes*-transformed roots of *Medicago truncatula* for the study of nitrogen-fixing and endomycorrhizal symbiotic associations. Mol. Plant Microbe Interact. **14:** 695–700.

Brandstatter, I., and Kieber, J.J. (1998). Two genes with similarity to bacterial response regulators are rapidly and specifically induced by cytokinin in *Arabidopsis*. Plant Cell **10:** 1009–1019.

Brenner, W.G., Romanov, G.A., Köllmer, I., Bürkle, L., and Schmülling, T. (2005). Immediate-early and delayed cytokinin response genes of *Arabidopsis thaliana* identified by genome-wide expression profiling reveal novel cytokinin-sensitive processes and suggest cytokinin action through transcriptional cascades. Plant J. **44:** 314–333.

Bustos-Sanmamed, P., Laffont, C., Frugier, F., Lelandais-Brière, C., and Crespi, M. (2012). Analyzing small and long RNAs in plant development using non-radioactive in situ hybridization. In Plant Organogenesis: Methods and Protocols (Methods in Molecular Biology), Vol. 959, I. De Smet, ed (New York: Humana Press), in press.

Carrere, S., and Gouzy, J. (2006). REMORA: A pilot in the ocean of BioMoby web-services. Bioinformatics **22:** 900–901.

Crooks, G.E., Hon, G., Chandonia, J.M., and Brenner, S.E. (2004). WebLogo: A sequence logo generator. Genome Res. **14:** 1188–1190.

D'Agostino, I.B., Deruère, J., and Kieber, J.J. (2000). Characterization of the response of the Arabidopsis response regulator gene family to cytokinin. Plant Physiol. **124:** 1706–1717.

Dello Ioio, R., Nakamura, K., Moubayidin, L., Perilli, S., Taniguchi, M., Morita, M.T., Aoyama, T., Costantino, P., and Sabatini, S. (2008). A genetic framework for the control of cell division and differentiation in the root meristem. Science **322:** 1380–1384.

Devers, E.A., Branscheid, A., May, P., and Krajinski, F. (2011). Stars and symbiosis: microRNA- and microRNA*-mediated transcript cleavage involved in arbuscular mycorrhizal symbiosis. Plant Physiol. **156:** 1990–2010.

Edgar, R.C. (2004). MUSCLE: Multiple sequence alignment with high accuracy and high throughput. Nucleic Acids Res. **32:** 1792–1797.

Ferguson, B.J., Ross, J.J., and Reid, J.B. (2005). Nodulation phenotypes of gibberellin and brassinosteroid mutants of pea. Plant Physiol. **138:** 2396–2405.

Frugier, F., Kosuta, S., Murray, J.D., Crespi, M., and Szczyglowski, K. (2008). Cytokinin: Secret agent of symbiosis. Trends Plant Sci. **13:** 115–120.

Godiard, L., Lepage, A., Moreau, S., Laporte, D., Verdenaud, M., Timmers, T., and Gamas, P. (2011). MtbHLH1, a bHLH transcription factor involved in Medicago truncatula nodule vascular patterning and nodule to plant metabolic exchanges. New Phytol. **191:** 391–404.

Gonzalez-Rizzo, S., Crespi, M., and Frugier, F. (2006). The *Medicago truncatula* CRE1 cytokinin receptor regulates lateral root development and early symbiotic interaction with *Sinorhizobium meliloti*. Plant Cell **18:** 2680–2693.

Greenboim-Wainberg, Y., Maymon, I., Borochov, R., Alvarez, J., Olszewski, N., Ori, N., Eshed, Y., and Weiss, D. (2005). Cross talk between gibberellin and cytokinin: The *Arabidopsis* GA response inhibitor SPINDLY plays a positive role in cytokinin signaling. Plant Cell **17:** 92–102.

Gruber, V., Blanchet, S., Diet, A., Zahaf, O., Boualem, A., Kakar, K., Alunni, B., Udvardi, M., Frugier, F., and Crespi, M. (2009). Identification of transcription factors involved in root apex responses to salt stress in *Medicago truncatula*. Mol. Genet. Genomics **281:** 55–66.

Heckmann, A.B., Lombardo, F., Miwa, H., Perry, J.A., Bunnewell, S., Parniske, M., Wang, T.L., and Downie, J.A. (2006). *Lotus japonicus* nodulation requires two GRAS domain regulators, one of which is functionally conserved in a non-legume. Plant Physiol. **142:** 1739–1750.

Hosoda, K., Imamura, A., Katoh, E., Hatta, T., Tachiki, M., Yamada, H., Mizuno, T., and Yamazaki, T. (2002). Molecular structure of the GARP family of plant Myb-related DNA binding motifs of the *Arabidopsis* response regulators. Plant Cell **14:** 2015–2029.

Hoth, S., Ikeda, Y., Morgante, M., Wang, X., Zuo, J., Hanafey, M.K., Gaasterland, T., Tingey, S.V., and Chua, N.H. (2003). Monitoring genome-wide changes in gene expression in response to endogenous cytokinin reveals targets in *Arabidopsis thaliana*. FEBS Lett. **554:** 373–380.

Hwang, I., and Sheen, J. (2001). Two-component circuitry in *Arabidopsis* cytokinin signal transduction. Nature **413:** 383–389.

Imamura, A., Kiba, T., Tajima, Y., Yamashino, T., and Mizuno, T. (2003). In vivo and in vitro characterization of the ARR11 response regulator implicated in the His-to-Asp phosphorelay signal transduction in *Arabidopsis thaliana*. Plant Cell Physiol. **44:** 122–131.

Ishida, K., Yamashino, T., Yokoyama, A., and Mizuno, T. (2008). Three type-B response regulators, ARR1, ARR10 and ARR12, play essential but redundant roles in cytokinin signal transduction throughout the life cycle of *Arabidopsis thaliana*. Plant Cell Physiol. **49:** 47–57.

Kaelin, W.G., Jr et al. (1992). Expression cloning of a cDNA encoding a retinoblastoma-binding protein with E2F-like properties. Cell **70:** 351–364.

Kaló, P., et al. (2005). Nodulation signaling in legumes requires NSP2, a member of the GRAS family of transcriptional regulators. Science **308:** 1786–1789.

Karas, B., Amyot, L., Johansen, C., Sato, S., Tabata, S., Kawaguchi, M., and Szczyglowski, K. (2009). Conservation of lotus and Arabidopsis basic helix-loop-helix proteins reveals new players in root hair development. Plant Physiol. **151:** 1175–1185.

Kiba, T., Aoki, K., Sakakibara, H., and Mizuno, T. (2004). *Arabidopsis* response regulator, ARR22, ectopic expression of which results in phenotypes similar to the *wol* cytokinin-receptor mutant. Plant Cell Physiol. **45:** 1063–1077.

Kiba, T., Naitou, T., Koizumi, N., Yamashino, T., Sakakibara, H., and Mizuno, T. (2005). Combinatorial microarray analysis revealing *Arabidopsis* genes implicated in cytokinin responses through the His->Asp phosphorelay circuitry. Plant Cell Physiol. **46:** 339–355.

Lee, D.J., Park, J.Y., Ku, S.J., Ha, Y.M., Kim, S., Kim, M.D., Oh, M.H., and Kim, J. (2007). Genome-wide expression profiling of *ARABIDOPSIS* RESPONSE REGULATOR 7(ARR7) overexpression in cytokinin response. Mol. Genet. Genomics **277:** 115–137.

Liu, Q., and Chen, Y.Q. (2009). Insights into the mechanism of plant development: Interactions of miRNAs pathway with phytohormone response. Biochem. Biophys. Res. Commun. **384:** 1–5.

Lohar, D.P., Schaff, J.E., Laskey, J.G., Kieber, J.J., Bilyeu, K.D., and Bird, D.M. (2004). Cytokinins play opposite roles in lateral root formation, and nematode and Rhizobial symbioses. Plant J. **38:** 203–214.

Lohrmann, J., Sweere, U., Zabaleta, E., Bäurle, I., Keitel, C., Kozma-Bognar, L., Brennicke, A., Schäfer, E., Kudla, J., and Harter, K. (2001). The response regulator ARR2: A pollen-specific transcription factor involved in the expression of nuclear genes for components of mitochondrial complex I in *Arabidopsis*. Mol. Genet. Genomics **265:** 2–13.

Madsen, L.H., Tirichine, L., Jurkiewicz, A., Sullivan, J.T., Heckmann A.B., Bek, A.S., Ronson, C.W., James, E.K., and Stougaard, J. (April 12, 2010). The molecular network governing nodule organogenesis and infection in the model legume *Lotus japonicus*. Nature Com. (online), doi/10.1038/ncomms1009.10.1038/ncomms1009

Maekawa, T., Maekawa-Yoshikawa, M., Takeda, N., Imaizumi-Anraku, H., Murooka, Y., and Hayashi, M. (2009). Gibberellin controls the nodulation signaling pathway in *Lotus japonicus*. Plant J. **58:** 183–194.

Marisa, L., Ichanté, J.L., Reymond, N., Aggerbeck, L., Delacroix, H., and Mucchielli-Giorgi, M.H. (2007). MAnGO: An interactive R-based tool for two-colour microarray analysis. Bioinformatics **23:** 2339–2341.

Mason, M.G., Mathews, D.E., Argyros, D.A., Maxwell, B.B., Kieber, J.J., Alonso, J.M., Ecker, J.R., and Schaller, G.E. (2005). Multiple type-B response regulators mediate cytokinin signal transduction in *Arabidopsis*. Plant Cell **17:** 3007–3018.

Mathesius, U., Charon, C., Rolfe, B.G., Kondorosi, A., and Crespi, M. (2000). Temporal and spatial order of events during the induction of cortical cell divisions in white clover by *Rhizobium leguminosarum* bv. *trifolii* inoculation or localized cytokinin addition. Mol. Plant Microbe Interact. **13:** 617–628.

Merchan, F., de Lorenzo, L., Rizzo, S.G., Niebel, A., Manyani, H., Frugier, F., Sousa, C., and Crespi, M. (2007). Identification of regulatory pathways involved in the reacquisition of root growth after salt stress in *Medicago truncatula*. Plant J. **51:** 1–17.

Middleton, P.H., et al. (2007). An ERF transcription factor in *Medicago truncatula* that is essential for Nod factor signal transduction. Plant Cell **19:** 1221–1234.

Murray, J.D., Karas, B.J., Sato, S., Tabata, S., Amyot, L., and Szczyglowski, K. (2007). A cytokinin perception mutant colonized by *Rhizobium* in the absence of nodule organogenesis. Science **315:** 101–104.

Oldroyd, G.E., and Downie, J.A. (2008). Coordinating nodule morphogenesis with rhizobial infection in legumes. Annu. Rev. Plant Biol. **59:** 519–546.

Oliphant, A.R., Brandl, C.J., and Struhl, K. (1989). Defining the sequence specificity of DNA-binding proteins by selecting binding sites from random-sequence oligonucleotides: Analysis of yeast GCN4 protein. Mol. Cell. Biol. **9:** 2944–2949.

Op den Camp, R.H., De Mita, S., Lillo, A., Cao, Q., Limpens, E., Bisseling, T., and Geurts, R. (2011). A phylogenetic strategy based on a legume-specific whole genome duplication yields symbiotic cytokinin type-A response regulators. Plant Physiol. **157:** 2013–2022.

Palena, C.M., Gonzalez, D.H., Guelman, S.A., and Chan, R.L. (1998). Expression of sunflower homeodomain containing proteins in *Escherichia coli*: Purification and functional studies. Protein Expr. Purif. **13:** 97–103.

Pichon, M., Journet, E.P., Dedieu, A., de Billy, F., Truchet, G., and Barker, D.G. (1992). *Rhizobium meliloti* elicits transient expression of the early nodulin gene *ENOD12* in the differentiating root epidermis of transgenic alfalfa. Plant Cell **4:** 1199–1211.

Plet, J., Wasson, A., Ariel, F., Le Signor, C., Baker, D., Mathesius, U., Crespi, M., and Frugier, F. (2011). MtCRE1-dependent cytokinin signaling integrates bacterial and plant cues to coordinate symbiotic nodule organogenesis in *Medicago truncatula*. Plant J. **65:** 622–633.

Quandt, H.J., Pühler, A., and Broer, I. (1993). Transgenic root nodules of *Vicia hirsuta*: A fast and efficient system for the study of gene expression in indeterminate-type nodules. Mol. Plant Microbe Interact. **6:** 699–706.

Rashotte, A.M., Carson, S.D.B., To, J.P.C., and Kieber, J.J. (2003). Expression profiling of cytokinin action in Arabidopsis. Plant Physiol. **132:** 1998–2011.

Rashotte, A.M., Mason, M.G., Hutchison, C.E., Ferreira, F.J., Schaller, G.E., and Kieber, J.J. (2006). A subset of *Arabidopsis* AP2 transcription factors mediates cytokinin responses in concert with a two-component pathway. Proc. Natl. Acad. Sci. USA **103:** 11081–11085.

Sakai, H., Aoyama, T., and Oka, A. (2000). *Arabidopsis* ARR1 and ARR2 response regulators operate as transcriptional activators. Plant J. **24:** 703–711.

Sakai, H., Honma, T., Aoyama, T., Sato, S., Kato, T., Tabata, S., and Oka, A. (2001). ARR1, a transcription factor for genes immediately responsive to cytokinins. Science **294:** 1519–1521.

Schauser, L., Roussis, A., Stiller, J., and Stougaard, J. (1999). A plant regulator controlling development of symbiotic root nodules. Nature **402:** 191–195.

Smith, D.B., and Johnson, K.S. (1988). Single-step purification of polypeptides expressed in *Escherichia coli* as fusions with glutathione *S*-transferase. Gene **67:** 31–40.

Stracke, R., Werber, M., and Weisshaar, B. (2001). The R2R3-MYB gene family in *Arabidopsis thaliana*. Curr. Opin. Plant Biol. **4:** 447–456.

Taniguchi, M., Sasaki, N., Tsuge, T., Aoyama, T., and Oka, A. (2007). ARR1 directly activates cytokinin response genes that encode proteins with diverse regulatory functions. Plant Cell Physiol. **48:** 263–277.

Tellström, V., Usadel, B., Thimm, O., Stitt, M., Küster, H., and Niehaus, K. (2007). The lipopolysaccharide of *Sinorhizobium meliloti* suppresses defense-associated gene expression in cell cultures of the host plant *Medicago truncatula*. Plant Physiol. **143:** 825–837.

Thimm, O., Bläsing, O., Gibon, Y., Nagel, A., Meyer, S., Krüger, P., Selbig, J., Müller, L.A., Rhee, S.Y., and Stitt, M. (2004). MAPMAN: A user-driven tool to display genomics data sets onto diagrams of metabolic pathways and other biological processes. Plant J. **37:** 914–939.

Tirichine, L., Sandal, N., Madsen, L.H., Radutoiu, S., Albrektsen, A. S., Sato, S., Asamizu, E., Tabata, S., and Stougaard, J. (2007). A gain-of-function mutation in a cytokinin receptor triggers spontaneous root nodule organogenesis. Science **315:** 104–107.

Truchet, G., Debellé, F., Vasse, J., Terzaghi, B., Garnerone, A.M., Rosenberg, C., Batut, J., Maillet, F., and Dénarié, J. (1985). Identification of a *Rhizobium meliloti* pSym2011 region controlling the host specificity of root hair curling and nodulation. J. Bacteriol. **164:** 1200–1210.

Ubeda-Tomás, S., Federici, F., Casimiro, I., Beemster, G.T., Bhalerao, R., Swarup, R., Doerner, P., Haseloff, J., and Bennett, M.J. (2009). Gibberellin signaling in the endodermis controls *Arabidopsis* root meristem size. Curr. Biol. **19:** 1194–1199.

Vandesompele, J., De Preter, K., Pattyn, F., Poppe, B., Van Roy, N., De Paepe, A., and Speleman, F. (2002). Accurate normalization of real-time quantitative RT-PCR data by geometric averaging of multiple internal control genes. Genome Biol. **3:** RESEARCH0034.

Varkonyi-Gasic, E., Wu, R., Wood, M., Walton, E.F., and Hellens, R.P. (2007). Protocol: A highly sensitive RT-PCR method for detection and quantification of microRNAs. Plant Methods **3:** 12.

Vernié, T., Moreau, S., de Billy, F., Plet, J., Combier, J.P., Rogers, C., Oldroyd, G., Frugier, F., Niebel, A., and Gamas, P. (2008). EFD Is an ERF transcription factor involved in the control of nodule number and differentiation in *Medicago truncatula*. Plant Cell **20:** 2696–2713.

Wasson, A.P., Pellerone, F.I., and Mathesius, U. (2006). Silencing the flavonoid pathway in *Medicago truncatula* inhibits root nodule formation and prevents auxin transport regulation by rhizobia. Plant Cell **18:** 1617–1629.

Welchen, E., and Gonzalez, D.H. (2005). Differential expression of the Arabidopsis cytochrome c genes Cytc-1 and Cytc-2. Evidence for the involvement of TCP-domain protein-binding elements in anther- and meristem-specific expression of the Cytc-1 gene. Plant Physiol. **139:** 88–100.

Werner, T., and Schmülling, T. (2009). Cytokinin action in plant development. Curr. Opin. Plant Biol. **12:** 527–538.

Yang, Y.H., Dudoit, S., Luu, P., Lin, D.M., Peng, V., Ngai, J., and Speed, T.P. (2002). Normalization for cDNA microarray data: A robust composite method addressing single and multiple slide systematic variation. Nucleic Acids Res. **30:** e15.

Zahaf, O., et al. (2012). Comparative transcriptomic analysis of salt adaptation in roots of contrasting Medicago truncatula genotypes. Mol. Plant **5:** 1068–1081.